DESIGN NOTE: DIFFRACTION EFFECTS

Original Author: John Rayner

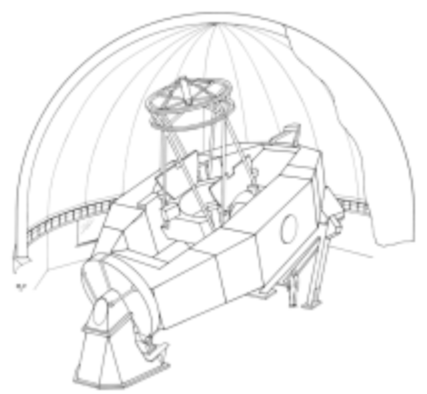

NASA Infrared Telescope Facility
Institute for Astronomy
University of Hawaii

Revision History

Revision No.	Author & Date	Approval & Date	Description
Revision 1	John Rayner 24 January 2011	John Rayner 24 January 2011	First release

Contents

1 INTRODUCTION

This design note will consider the effects of diffraction due to the relatively small slit width and relatively small size of the immersion gratings in the spectrograph, coupled with the requirement to optimize performance at 3-5 μm.

In the simplest possible configuration the spectrograph comprises a collimator-camera configuration. The f/38 beam from the telescope is focused onto the slit that is placed at the front focus of the collimator, and the telescope pupil is imaged one focal length behind the collimator. This is usually the location of the grating and spectrograph pupil stop (smallest collimated beam diameter). The function of the pupil stop is to prevent light from outside the optical beam from scattering into the spectrograph and onto the spectrograph detector. This is done by placing an aperture matched to the size the telescope pupil at the re-imaged pupil. In a simple re-imaging system this works very well. However, in a spectrograph the effect of a narrow slit is to blur the image of the pupil due to diffraction at the slit, creating a path for light outside the optical beam into the spectrograph. We model this effect in Section 2 and conclude that for this and other reasons it is best to form an optimized cold stop in front of the spectrograph.

If geometrical aberrations are minimized the spectrograph instrument profile is the result of convolving the rectangular slit profile with the diffraction profile of the limiting aperture in the spectrograph. In an ideal instrument the limiting aperture is large enough that diffraction effects are insignificant and the image of the slit on the detector is sharp. In iSHELL the aperture at the immersion grating is small by design (about 30 mm) to keep the instrument small and the slit image is blurred by diffraction at immersion grating aperture. Note that this effect is different to diffraction due from the telescope aperture D ($\sim\lambda/D$). Diffraction due to the small immersion-grating aperture is modeled in Section 3 and mitigating measures discussed in Section 4.

2 DIFFRACTION AT THE SPECTROGRAPH SLIT

Diffraction at the slit is modeled using the simplified model of the iSHELL spectrograph shown in Figure 1. The f/38.1 beam from the telescope is focused onto the slit and the slit is re-imaged onto the detector at a demagnification of 3.81 with a paraxial collimator and paraxial camera of focal lengths 838 mm and 220 mm respectively (f/10.0 onto the detector). A 22.0 mm diameter image of the telescope pupil is formed one focal length (838 mm) behind the collimator as shown. This is the location of the conjugated pupil image (stop) and immersion grating.

Figure 2 shows the image of the telescope entrance pupil at a wavelength of 4.8 μm (upper) when the slit is wide open. As expected the image is sharp and all the energy is contained within the geometrical diameter of 22.0 mm (lower) since the slit aperture is not close to the point source in the focal plane – equivalent to a simple imager.

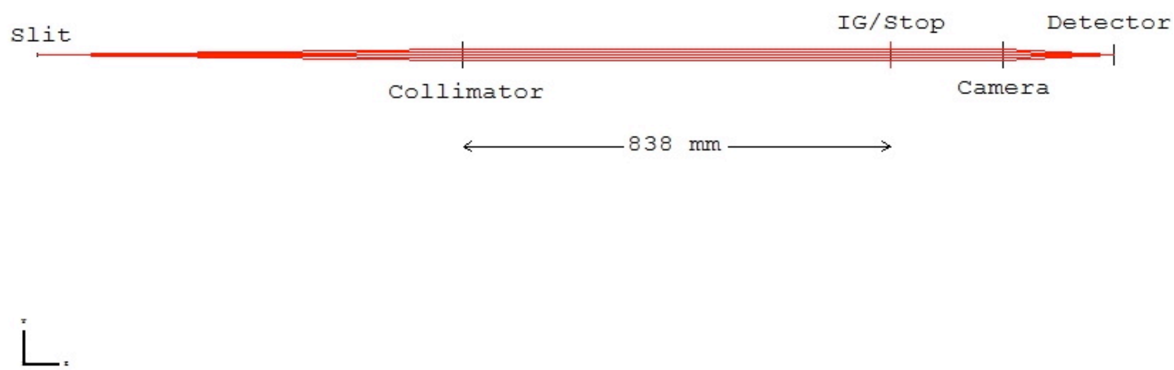

Figure 1. A simplified collimator-camera model of the spectrograph. The slit is re-imaged onto the detector and an image of the telescope pupil is formed at the immersion grating (IG).

Figure 3 shows the image of the telescope entrance pupil at a wavelength of 4.8 μm (upper) with the narrowest slit in the focal plane (0.208 mm × 8.4 mm – equivalent to 0.375″ × 15.0″). The image of the telescope entrance pupil now becomes blurred in the narrow direction (x) but still sharp in the long direction (y). As a consequence the x-enslitted energy within the geometrical diameter of 22.0 mm is reduced from 1.0 to about 0.85 due to diffraction at the narrow slit. (The effect is less at 2.2 μm where the x-enslitted energy is reduced to 0.95.) This is equivalent to an emissivity of 0.15 and given the telescope emissivity of about 0.05 results in a total emissivity at 4.8 μm of 0.20, a four fold increase over a perfectly optimized stop. Together with the increase in emissivity the un-sharp stop will also result in light outside the optical beam scattering into the spectrograph and onto the detector.

To avoid these effects a better approach is to form an optimized pupil in front of the slit and place the instrument cold stop there. Consequently iSHELL will have a simple collimator-camera in front of the spectrograph to re-image the f/38.1 telescope focal plane onto the slit plane and form a sharp 10.0 mm diameter image of the telescope entrance pupil on a cold stop. Placing a small pupil in the fore-optics also greatly simplifies the design of the internal k-mirror field rotator.

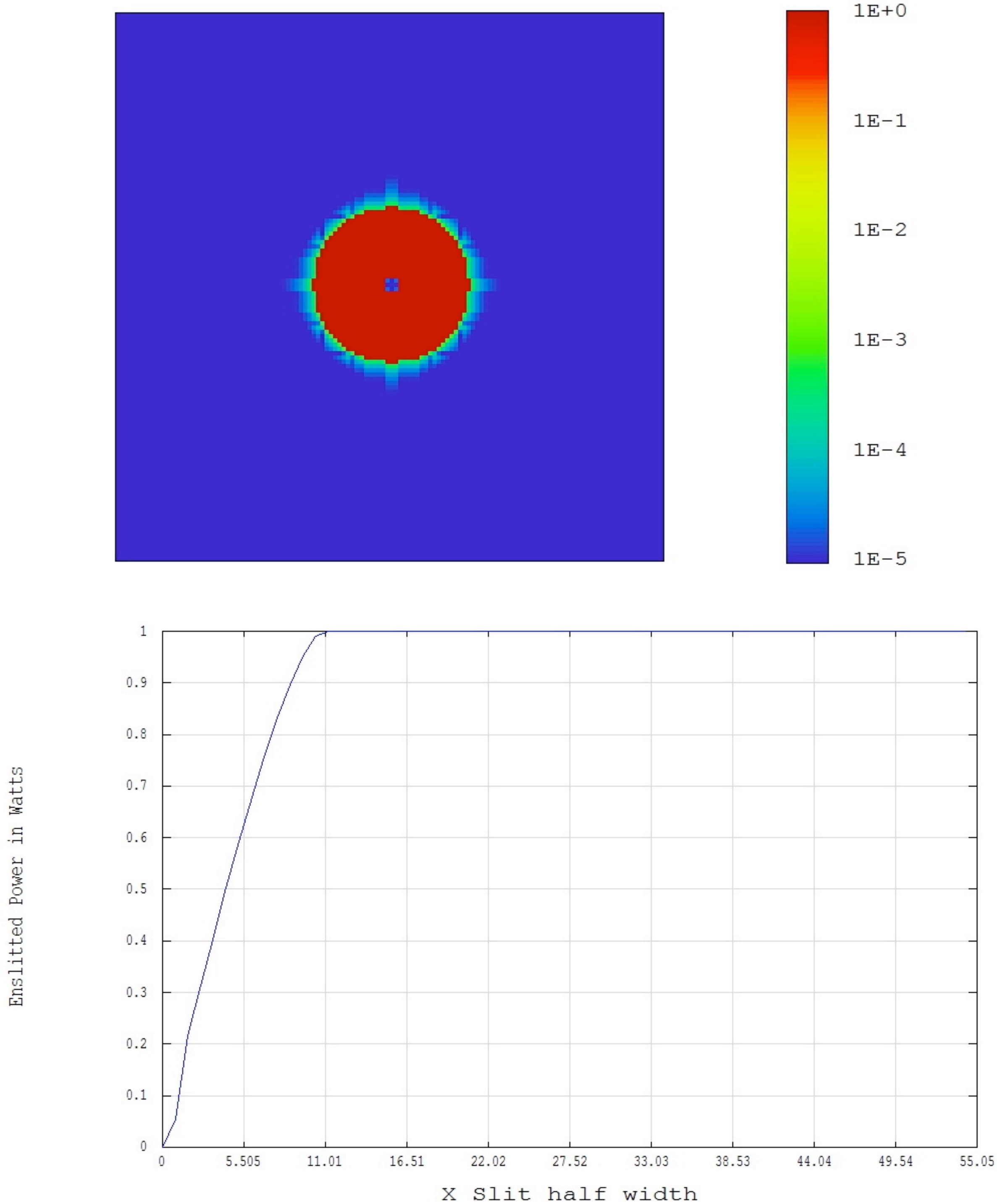

Figure 2. Image of the telescope pupil at 4.8 µm (including the primary hole) with the slit wide open (*top*). Enslitted energy (*bottom*). All the energy is contained within the geometrical diameter of 22.0 mm. The total intensity has been normalized to one watt.

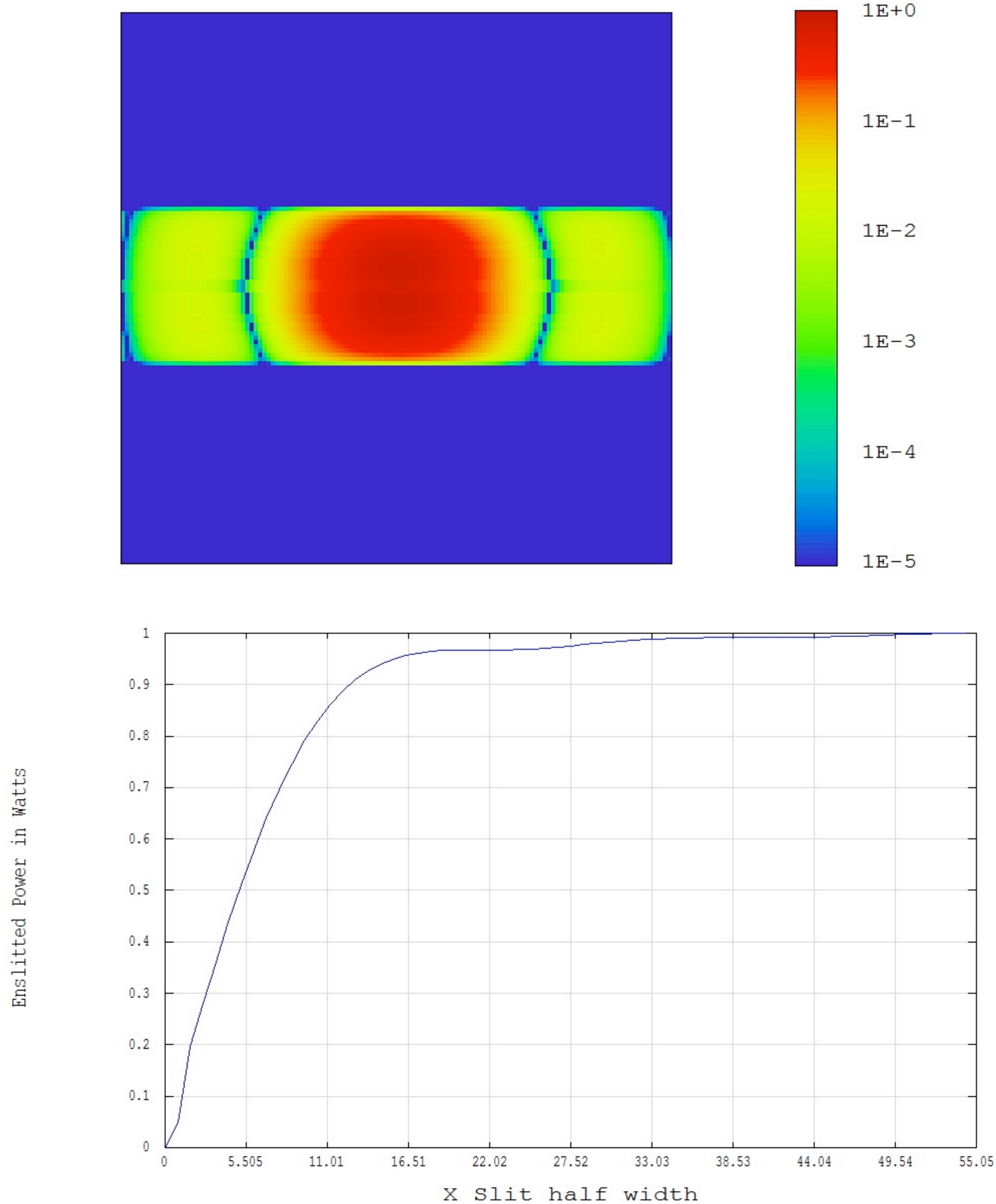

Figure 3. Image of the telescope pupil at 4.8 μm (including the primary hole) with the slit wide open (*top*). Enslitted energy (*bottom*). All the energy is contained within the geometrical diameter of 22.0 mm. The total intensity has been normalized to one watt.

3 DIFFRACTION AT THE IMMERSION GRATING APERTURE

If geometrical aberrations are minimized the spectrograph instrument profile is the result of convolving the rectangular slit profile with the diffraction (Airy sinc) profile of the limiting aperture in the spectrograph. In an ideal instrument the limiting aperture is large enough that diffraction effects are insignificant and the image of the slit on the detector is sharp. In iSHELL the aperture at the immersion grating is small by design (about 30 mm) to keep the instrument small, and the slit image is blurred by diffraction at immersion grating aperture.

The intensity in the dispersion direction (x at the detector array) is given by:

$$\prod_a * A_o^2 \left[\frac{\sin\beta}{\beta}\right]^2 \quad \textbf{(1)}$$

where the top hat function $\prod = 0,\ -\infty < x < -a/2$
$= 1,\ -a/2 < x < a/2$
$= 0,\ a/2 < x < \infty$

* represents the convolution
a is the width of the re-imaged slit (3 pixels or 54 μm)
A_0 is the amplitude of the Airy function
$\beta = \frac{\pi}{\lambda}\frac{b}{f}x$ for small x
b is the size of the aperture in direction x (30.5 mm)
f is the focal length of the camera lens (220 mm)

The convolution is coded in IDL and the results compared to the Physical Optics Propagation (POP) package in the Zemax sequential raytrace.

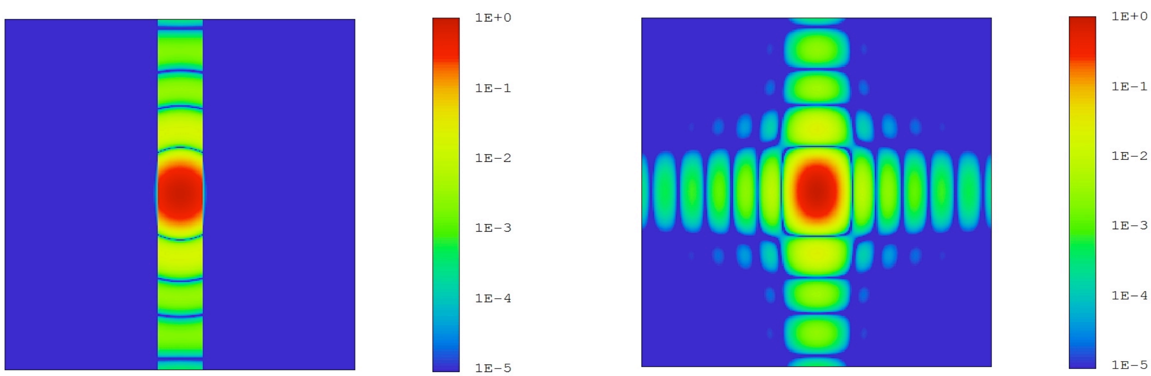

Figure 4. (*Left*) 4.8 μm image of the slit at the array with a star focused onto the slit and with a large aperture at the pupil/immsersion grating. The slit image is perfect. The Airy pattern of the star along the slit is due to diffraction of the telescope. (*Right*) Same image but now with the aperture at the pupil/immersion grating reduced to a 30.5 mm x 35.0 mm rectangle (immersion grating face). Diffraction at this aperture leads to the spreading of the instrument profile.

Figure 4 shows the results of the POP analysis at 4.8 μm and how diffraction from the small aperture at the immersion grating broadens the instrument profile in the dispersion direction. It is interesting to note that little extra broadening results in the spatial (i.e. cross dispersion) direction since this profile is just the Airy point source profile resulting from the telescope pupil (matched to 22.0 mm diameter at the reimaged pupil/immersion grating) and so the aperture of the immersion grating is already larger than the pupil in this direction.

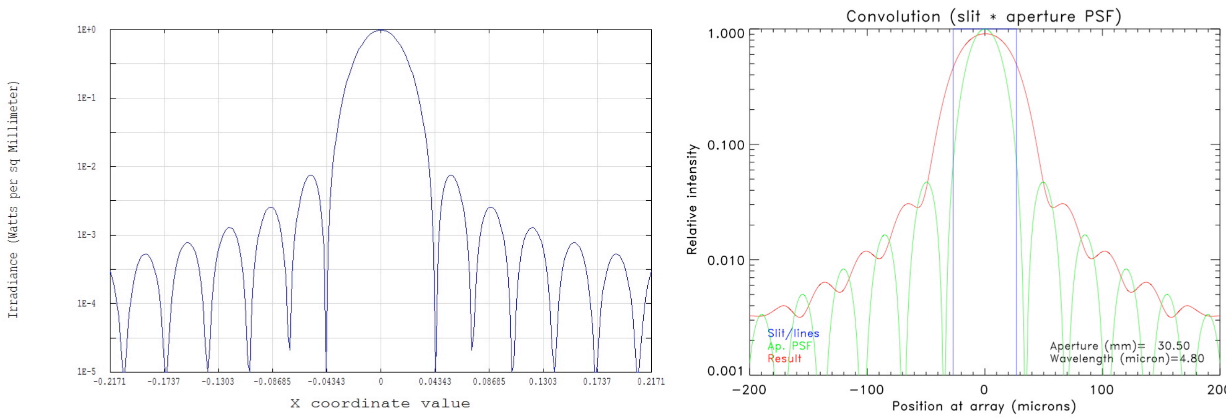

Figure 5. (*Left*) The intensity profile in the dispersion direction (x in mm at the array) plotted from Figure 4 (right). (*Right*) The calculated instrument profile from Equation 1 (x in microns at the array). The FWHM of both profiles is the same and equal to the FWHM of the re-imaged slit onto the array, however the calculation indicated that slightly more flux is scattered into the wings of the instrument profile.

Figure 5 compares the calculated instrument profile from Equation 1 at 4.8 μm with the POP analysis. The results are similar except that the calculated profile indicates that slightly more flux is scattered into the wings of the instrument profile. The difference is probably due to slightly different flux distributions in the slit. The POP analysis uses a truncated point source (see Figure 4) while the calculation use a uniform top-hat distribution. In practice, the more uniform distribution is a better match to seeing and guiding errors. The FWHM of the resulting profile is the same as a perfectly re-imaged slit and so the basic resolving power of the spectrograph is not degraded. However, because more flux is scattered into the wings of the profile feature contrast is reduced with increasing wavelength and feature density as illustrated in Figures 6-9.

In the simulation the spectral features are represented by a series of top hot functions one slit width wide and separated by half a slit width (center to center 4.5 pixels, equivalent to a resolving power of R=53,333). Diffraction at the immersion-grating aperture degrades the line contrast (maximum relative intensity minus minimum relative intensity all divided by maximum relative intensity) from about 0.9 at 1.25 μm to 0.5 at 4.8 μm (right hand plots of Figures 6-9). In a perfect iSHELL the contrast would be 1.0 with little separation between the features (center to center 3 pixels, equivalent to R=80,000). Since it is not possible to increase the aperture of the immersion grating the only way to improve the line contrast is to increase the separation between spectral features, which is done by increasing the dispersion (see Section 4.3).

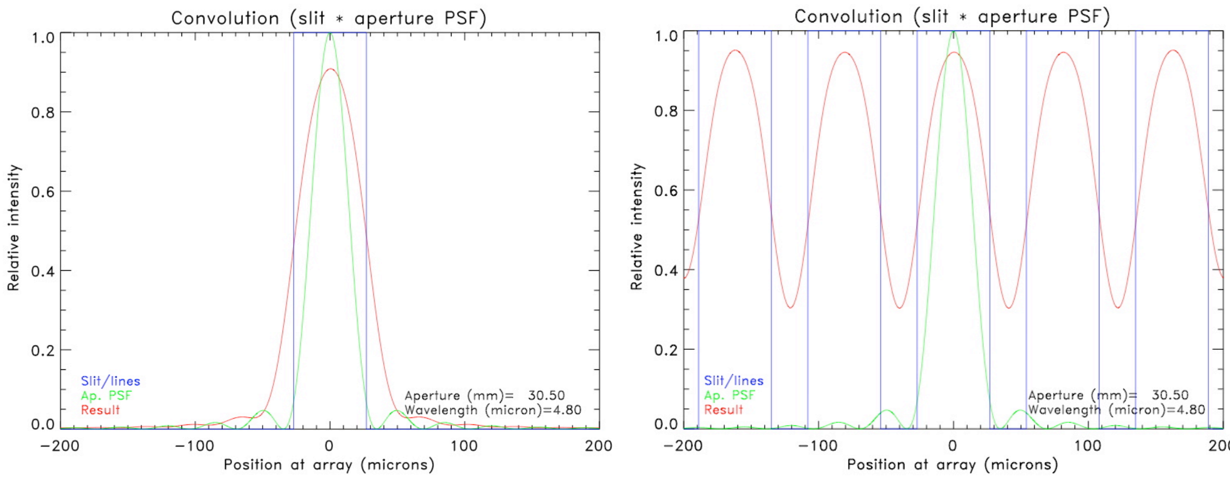

Figure 6. (*Left*) The instrument profile at 4.8 µm. (*Right*) With spectral features separated by half a slit width (equivalent to R=53,333) the feature/line contrast is degraded to 0.5 (red) from the perfect instrument profile of 1.0 (blue) due to diffraction at the immersion grating aperture of 30.5 mm x 35.0 mm (green).

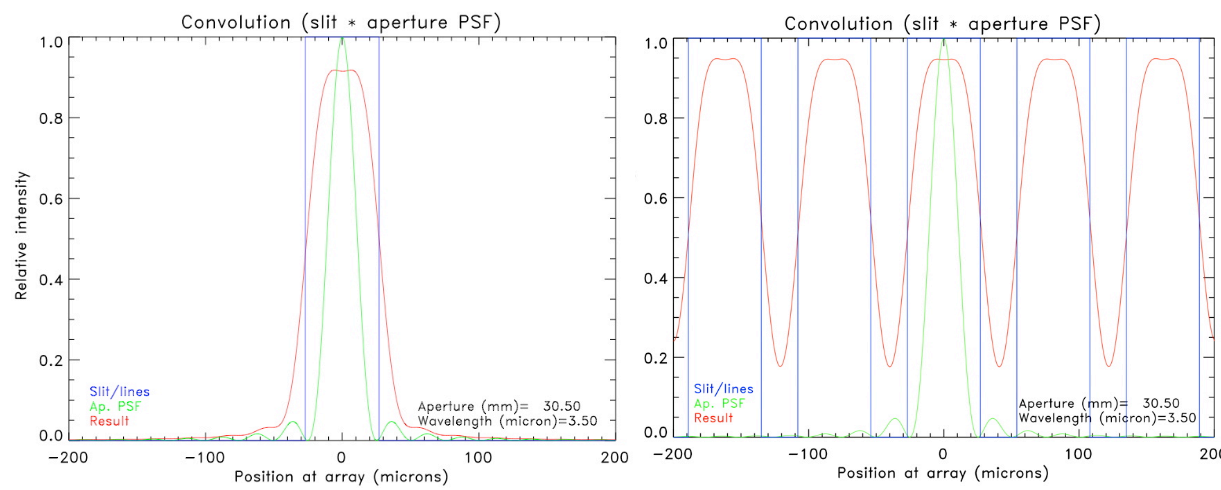

Figure 7. (*Left*) The instrument profile at 3.5 µm. (*Right*) With spectral features separated by half a slit width (equivalent to R=53,333) the feature/line contrast is degraded to 0.75 (red) from the perfect instrument profile of 1.0 (blue) due to diffraction at the immersion grating aperture of 30.5 mm x 35.0 mm (green).

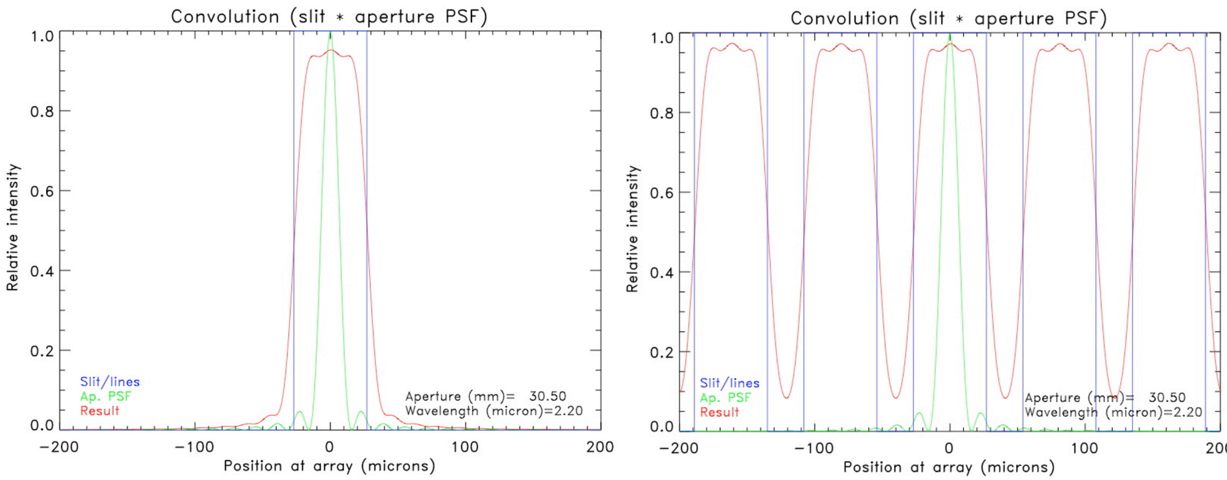

Figure 8. (*Left*) The instrument profile at 2.2 µm. (*Right*) With spectral features separated by half a slit width (equivalent to R=53,333) the feature/line contrast is degraded to 0.85 (red) from the perfect instrument profile of 1.0 (blue) due to diffraction at the immersion grating aperture of 30.5 mm x 35.0 mm (green).

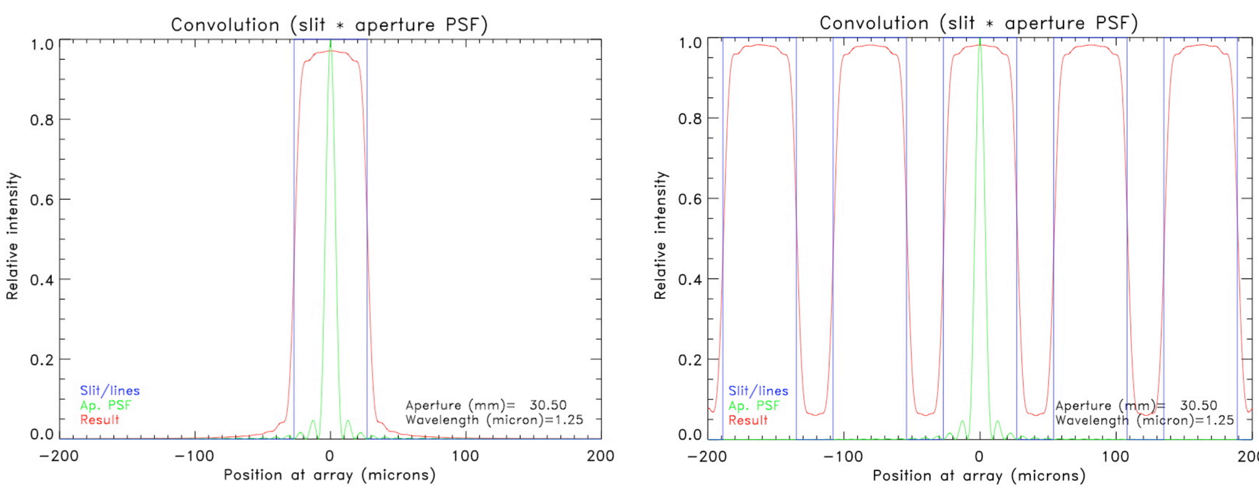

Figure 9. (*Left*) The instrument profile at 1.25 µm. (*Right*) With spectral features separated by half a slit width (equivalent to R=53,333) the feature/line contrast is degraded to 0.9 (red) from the perfect instrument profile of 1.0 (blue) due to diffraction at the immersion grating aperture of 30.5 mm x 35.0 mm (green).

4 MITIGATING MEASURES FOR iSHELL

In this section we propose mitigating measures for the diffraction effects discussed above. These measures also come at a cost and so the trade-offs are also considered.

4.1 Put cold stop in front of slit

Diffractive blurring of a pupil placed behind the slit results in an increase in emissivity and scattered light. The best solution is to form an optimized pupil stop in front of the slit by employing a simple collimator-camera re-imaging system. This also has the very significant advantage of providing a small pupil (10.0 mm diameter) at which an internal field rotator can be placed, which would otherwise be much larger and difficult to build. The disadvantage of the fore-optics is the added complication and loss of throughput (i.e. signal) but the reduction in noise (i.e. emissivity and scattered light) is more significant and overall S/N is improved.

4.2 Maximize immersion grating and cross-disperser grating apertures

As demonstrated above, the relatively small aperture (30.5 mm x 35.0 mm) of the silicon immersion grating entrance/exit face results in diffraction that scatters flux into the wings of the instrument profile and reduces the contrast of spectral features. As a practical matter it is not possible to increase the size of the immersion-grating entrance/exit aperture any further due to the size of the silicon boule that the University of Texas uses. Since the immersion grating and cross-dispersing gratings are placed at same size conjugate pupils in the spectrograph, the cross-dispersing gratings should be of at least this size (normal to the optical beam).

4.3 Oversize optical baffles in the spectrograph

Optical baffles in the spectrograph need to be oversized to take into account the larger effective beam consistent with the beam shape of 30.5 mm x 35.0 mm projected from the immersion grating towards the slit and towards the detector and not the 22.0 mm diameter collimated beam.

4.4 Increase dispersion at 3-5 μm

The degradation in the contrast of spectral features becomes significant in the 3-5 μm mode. One way to mitigate the effect is to move the features further apart by increasing the spectral dispersion. In iSHELL the free spectral range (FSR) in the longest wavelength L' spectral order (m) is matched to the width of the H2RG array. From this it follows that:

$$FSR = \frac{\lambda_c}{R \times s} span \quad (2)$$

where λ_c is the central wavelength of the spectral order
R is the resolving power (80,000) matched to the slit, s, in pixels at the array
s is also known as the the sampling in pixels (3)
span is the useable width of the array in pixels (2000)

Also, since FSR = λ_c / m, it follows that:

$$m = \frac{R \times s}{span} \quad (3)$$

Spectral feature contrast can be improved by increasing the slit width at the array (s) since the flux scattered into the wings of the instrument profile is then a smaller proportion of the slit width. From Equation 3 this means working in higher order (m). This is done by using a coarser grating since the groove width is given by:

$$\sigma = \frac{m\lambda_c}{2n\sin\delta} \quad (4)$$

for an immersion grating of refractive index, n, and blaze angle, δ, used in near Littrow.

The disadvantage of working in higher orders is the reduction in simultaneous wavelength coverage due to the reduced FSR range. Also, the cross-dispersing gratings have to work at higher blaze angle, β_x, for a given slit length, since:

$$\tan\beta_x = \frac{mw}{2f_c} \quad (5)$$

where w is the linear separation of the spectral orders (i.e. slit length)
f_c is the focal length of the spectrograph camera

For example, increasing the sampling from 3 pixels to 4.5 pixels improves the feature contrast from 0.5 to 0.8 (see Figure 10) for features separated by 9 x10^{-5} μm at 4.8 μm (equivalent to

R=53,333). The order increases from m=120 to m=180 for the order spanning the array (λ_c=4.1µm), and the groove width increases from 80 µm to 120 µm, with a corresponding reduction of 33% in the FSR.

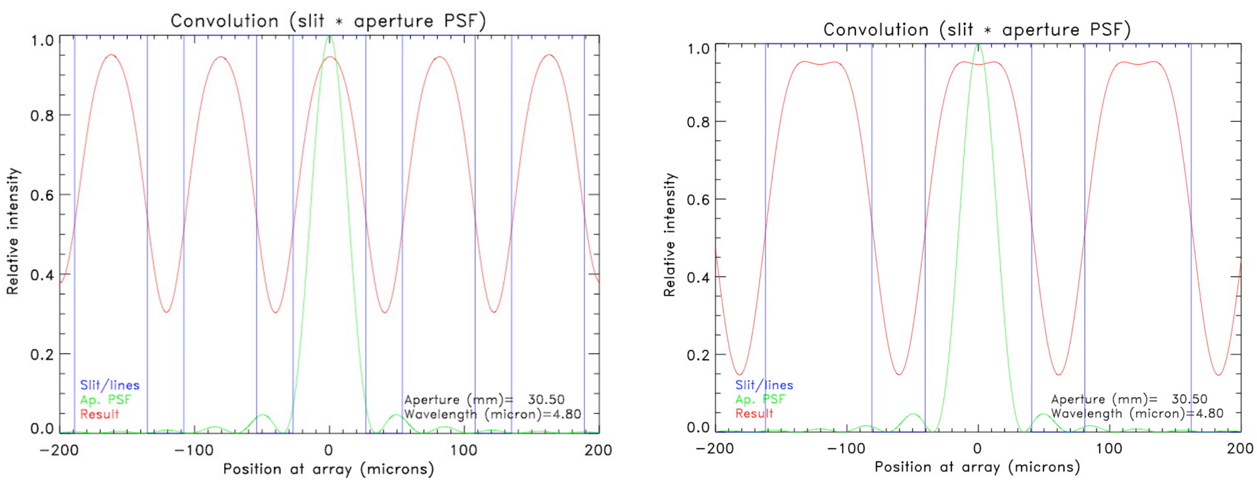

Figure 10. (*Left*) Feature contrast at 4.8 µm with R=80,000 matched to 3 pixels. (*Right*) Feature contrast at 4.8 µm with R=80,000 matched to 4.5 pixels. The contrast improves from 0.5 to 0.8.

For most iSHELL science programs the reduction in FSR (and therefore total one-shot wavelength coverage) by 33% at 3-5 is not a concern (an exception is the spectral library project). Of more concern is the required increases in cross-disperser blaze angle (see Equation 5) since the cross-disperser gratings already have to operate at relatively high blaze angles (up to 45 degrees) due to the small collimated-beam diameter (22 mm). Operating at yet higher blaze angles could also be a source of increased scatter and reduction in spectral feature contrast, negating the desired fix. However, this is more difficult to model.

Where spectral features cannot be separated due to the noise RMS having the same amplitude as the contrast, the features can be resolved by increasing the contrast, or by reducing noise by integrating longer. For example, improving contrast by a factor of two is equivalent to increasing S/N by the same factor. For photon-limited observations this is achieved by increasing the integration time by 2^2 (if systematic effects do not limit S/N). To improve contrast for high S/N data it should be possible to measure the instrument profile and remove it.

From Figures 6-9 it is apparent that degraded contrast becomes significant in the measurement of crowded spectral features at wavelengths longer than about at 4 µm. Given the risk of using higher angle blaze cross-dispersing gratings, we conclude that the best solution for iSHELL is to improve the S/N or remove the instrument profile for observations that require it.